Second International Conference on CFD in the Minerals and Process Industries
CSIRO, Melbourne, Australia
6-8 December 1999

COMPUTATIONAL FLUID DYNAMICS MODELLING OF IRON FLOW AND HEAT TRANSFER IN THE IRON BLAST FURNACE HEARTH

Vladimir PANJKOVIC[1] and John TRUELOVE[2]

[1] formerly: Steel Research Laboratories, BHP Steel, PO Box 202, Port Kembla NSW 2505, AUSTRALIA
now: BHP Information Technology, Level 32, 600 Bourke St., Melbourne VIC 3000, AUSTRALIA
[2] Centre for Metallurgy and Resource Processing, BHP Minerals, PO BOX 188, Wallsend NSW 2287, AUSTRALIA

ABSTRACT

The erosion of hearth refractories significantly limits the life of a blast furnace. The design of control strategies for refractory wear reduction is facilitated by the use of computational modelling, which, in this case, provides an attractive tool for understanding the fluid flow and heat transfer conditions within the hearth. A computational fluid dynamics model of the iron flow and heat transfer in the hearth has been developed using the commercial package CFX 4.2. It calculates the iron flow pattern and the temperature profiles in the liquid iron and the hearth refractories, which is essential for estimation of wear rate under various operational regimes. The model has been extensively evaluated using thermocouple measurements from the hearth of BHP's Port Kembla No. 5 Blast Furnace, and the agreement between the measured and calculated data is satisfactory. The model is now actively used for analysis of hearth conditions.

NOMENCLATURE

C_k	constant in turbulent viscosity formula (=1.224)
C_{lm}	constant in turbulent viscosity formula (=0.0413)
C_μ	constant in turbulent viscosity formula (=0.09)
C_p	heat capacity
d	coke diameter
g	gravitational constant
H	enthalpy
p	pressure
Re	Reynolds number
S_u	resistance to flow through porous medium
T	temperature
$\boldsymbol{u}$	interstitial velocity
β	coefficient of volumetric thermal expansion
ε	porosity
λ	thermal conductivity
μ_{eff}	effective viscosity
μ_L	laminar viscosity
μ_T	turbulent viscosity
ρ	density

INTRODUCTION

The iron blast furnace is a counter-current reactor, where iron ore, coke and fluxes are charged from the top, while hot air and other injectants are blown in through tuyeres. Burning of coke and auxiliary fuels provides heat for melting of ore and gases for reduction of iron oxides. The molten iron and slag accumulate in the hearth, where they percolate through packed unburnt coke ("deadman") and are tapped via a taphole.

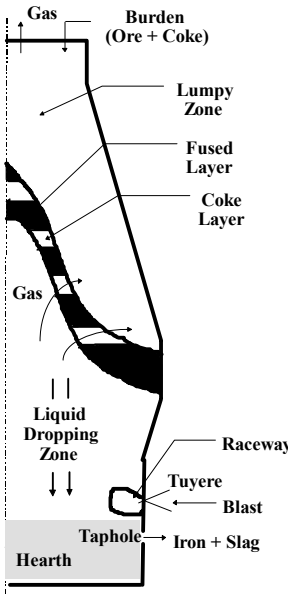

Figure 1: Schematic of the ironmaking blast furnace.

Extension of a blast furnace campaign requires effective control of the hearth wear. This, in turn, requires knowledge of the fluid flow and heat transfer in the hearth to estimate the wear under various operational regimes and to devise new control strategies. To obtain this information by plant trials is impractical and there is a considerable interest in the use of computational modelling.

The modelling of the hearth is complicated. The model has to address conjugate heat transfer, natural convection, flow through porous medium and the wide range of geometry and velocity scales. For the furnaces at BHP Port Kembla steelworks, the taphole diameter is 6-15 cm and the hearth diameter is over 10 m, while iron velocities range from several meters per second to a fraction of a millimetre per second. Several interesting hearth models have been reported in the literature, but it was still necessary to develop a proprietary model since they had significant shortcomings. Yoshikawa and Szekely (1981),

Preuer et al. (1992), Kurita and Ogawa (1994) and Kowalski et al. (1998) reported models which did not explicitly include refractory walls. Leprince et al. (1993), Tomita and Tanaka (1994) and Venturini et al. (1998) included refractories, but ignored natural convection. The model of Shibata et al. (1990) was quite comprehensive and was evaluated to some extent (calculated temperatures in the refractories were compared to actual thermocouple readings). However, the results were obtained on a crude grid of 820 nodes. A comprehensive model was reported by Iwamasa et al. (1997). Refractory walls and natural convection were included, and refined grid was used (113,500 nodes). The Iwamasa model has been revised and enhanced; a description of the current model is provided below.

MODEL DESCRIPTION

General Features

This model has been developed using the commercial CFD package, CFX 4.2. It is a three-dimensional, finite volume model with collocated grid. A body-fitted H-grid with Cartesian coordinates is used and consists of 148,770 control volumes (Fig. 2). The geometry is based on BHP's Port Kembla No.5 Blast Furnace (PK5BF). Model parameters are listed in Table 1.

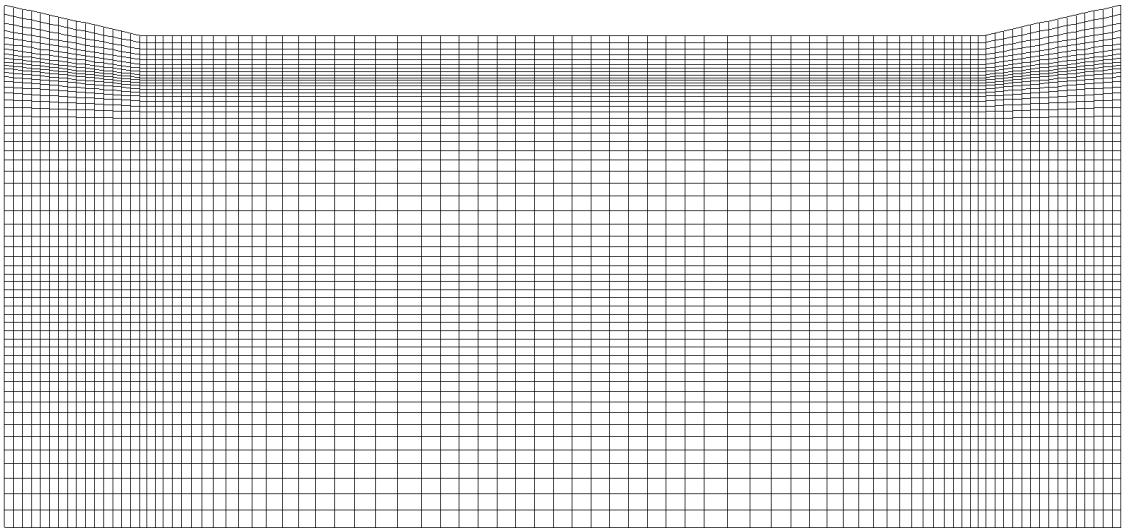

Figure 2: The projection of grid on the symmetry plane.

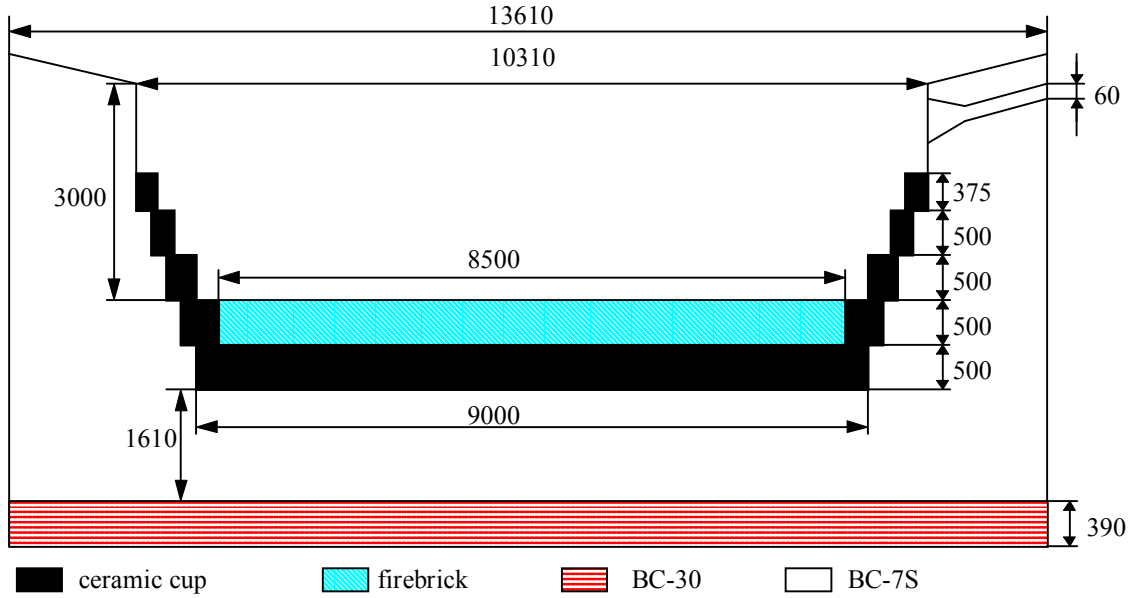

Figure 3: Basic dimensions of computational domain [in mm] and the layout of refractories (not to scale). The top surface of refractories is slanted to allow representation of inclined taphole (12.5^{o}).

Iron	
Laminar viscosity	0.00715 Pa s
Thermal conductivity	16.5 W m^{-1} K^{-1}
Heat capacity	850 J kg^{-1} K^{-1}
Density	7000 kg m^{-3}
Thermal coefficient of volumetric expansion	$1.4x10^{-4}$ K^{-1}
Production rate	80 kg s^{-1}
Height of liquid above the top of taphole entrance	0.25 m
Refractories	
Heat capacity	1260 J kg^{-1} K^{-1}
Thermal conductivity of BC-7S[1)]	12.0 W m^{-1} K^{-1} , T ≤ 30°C 13.5 W m^{-1} K^{-1} , T = 400°C 15.5 W m^{-1} K^{-1} , T ≥ 1000°C
Thermal conductivity of BC-30	38 W m^{-1} K^{-1}
Thermal conductivity of firebrick[1)]	2.38 W m^{-1} K^{-1} , T ≤ 800°C 2.31 W m^{-1} K^{-1} , T ≥ 1200°C
Thermal conductivity of ceramic cup[1)]	2.20 W m^{-1} K^{-1} , T ≤ 400°C 2.00 W m^{-1} K^{-1} , T = 500°C 2.05 W m^{-1} K^{-1} , T = 600°C 2.15 W m^{-1} K^{-1} , T = 800°C 2.20 W m^{-1} K^{-1} , T = 1000°C 2.30 W m^{-1} K^{-1} , T = 1200°C 2.35 W m^{-1} K^{-1} , T ≥ 1400°C
Coke bed	
Particle diameter	0.03 m
Porosity	0.35

1) Conductivity is assumed to change linearly between discrete temperature values.

Table 1: Standard values of model parameters.

Assumptions

1. The process is steady state;
2. The free surface of liquid iron is flat and horizontal;
3. The presence of slag is neglected;
4. Chemical reactions and solidification are neglected;
5. The coke bed and the iron are at the same temperature; and
6. Taphole is coke-free.

Boundary Conditions

The following boundary conditions are imposed:

1. The liquid iron level is constant;
2. The free surface of the liquid iron is an inlet boundary with fixed temperature;
3. The inlet velocity of liquid iron is uniform over this iron surface;
4. No-slip conditions exist on the hot face of refractory walls;
5. No mass transfer occurs between liquid iron and refractory walls;
6. The top surface of the refractory walls is adiabatic;
7. The taphole exit is a mass flow boundary;
8. Cold faces of refractories are set as conducting boundaries; and
9. The vertical cross-section defined by the centreline of the taphole and the centreline of the hearth is a symmetry plane.

The code ensures continuity of temperature and heat flux between the liquid iron and the refractory walls. Momentum and enthalpy (Jayatilleke) wall functions are used to implement the boundary conditions for flow and heat transfer at walls (CFX 4.2, 1997).

CFX Options

Model performance strongly depends on the selection of CFX options (CFX 4.2, 1997). The following setup was found to eliminate the mass imbalance, hot spots and spurious vectors:

1. Rhie-Chow switch with the modified resistance treatment;
2. Two iterations of the temperature and scalar equation;
3. PISO pressure correction with two correction steps;
4. Algebraic multigrid solver for pressure and enthalpy;
5. The hybrid differencing scheme; and
6. The discretised equations for momentum are solved using Stone's method.

Conservation Equations

The mass conservation and the momentum transport equations are given by:

$$\nabla \bullet \left(\rho \, \boldsymbol{u} \right) = 0 \tag{1}$$

$$\begin{aligned} &\nabla \bullet \left(\rho \, \boldsymbol{u} \times \boldsymbol{u} - \mu_{eff} \nabla \boldsymbol{u} \right) \\ &= -\nabla p + \nabla \bullet \left(\mu_{eff} (\nabla \boldsymbol{u})^T \right) + S_u + g\rho\beta \left(T - T_{ref} \right) \end{aligned} \tag{2}$$

The criteria set out by Gray and Giorgini (1976) indicate that the Boussinesq approximation is valid for these simulations. The effective viscosity is calculated as the sum of the laminar and turbulent viscosities:

$$\mu_{eff} = \mu_L + \mu_T \tag{3}$$

while the resistance to flow through the coke bed is calculated using Ergun's equation:

$$S_u = -150\mu_L \frac{(1-\varepsilon)^2}{\varepsilon^2 d^2} |\boldsymbol{u}| - 1.75\rho \frac{1-\varepsilon}{\varepsilon \, d} |\boldsymbol{u}|^2 \tag{4}$$

In packed beds the dimension of eddies depends on the distance between particles, and the k-ε model cannot be applied directly. The modified k-ε model suggested by Sha et al. (1982) made the whole model prohibitively slow. In the current model, turbulent viscosity in the deadman is calculated using the formula proposed by Takeda (1994):

$$\mu_T = C_\mu C_k^{1/3} C_{lm}^{4/3} \rho \, |\boldsymbol{u}| \frac{\varepsilon \, d}{1-\varepsilon} \left[\frac{150(1-\varepsilon)}{\mathrm{Re}} + 1.75 \right]^{1/3} \tag{5}$$

The transport equation for enthalpy is given by:

$$\nabla \bullet \left(\rho \, \boldsymbol{u} H - \left(\frac{\lambda}{C_P} + \frac{\mu_T}{0.9} \right) \nabla H \right) = 0 \tag{6}$$

RESULTS

The typical results obtained with the model are best illustrated with the flow pattern of liquid iron (Fig. 4) and the temperature contours in the liquid iron and refractories

(Fig. 5). These results are obtained with the standard data set and the refractory profile at the beginning of campaign. The recirculation loops caused by natural convection are clearly visible in the lower half of the fluid domain (on the right hand side) and just above the refractory steps on the left hand side. The stratified temperature of liquid iron is consistent with significant buoyancy forces.

Evaluation of the Model

The model has been extensively evaluated using thermocouple measurements at PK5BF. The furnace was relined in 1991 and is well equipped with thermocouples in the pad and sidewalls. Four sidewall thermocouples and twenty pad thermocouples were used for evaluation, and their positions can be seen in Fig. 6. There were two interesting periods for evaluation, before the erosion of firebrick and some sidewall refractories in 1995 and after it. The evidence for erosion of the firebrick was obtained from the pad thermocouples, where a sudden increase in temperature was observed, and the temperature never returned to the previous level. Regarding the sidewalls, during the same period temperatures at three different heights which were previously clearly different, became very similar in magnitude. Using the readings of sidewall thermocouples inserted 40 mm into the carbon bricks, and the pad thermocouples located 300 mm above the bottom and 100 mm under the bottom, the boundary temperatures were set at:

- 70^{o}C at the sidewall and 80^{o}C at the bottom (intact refractories);
- 80^{o}C at the sidewall and 100^{o}C at the bottom (firebrick and some sidewall refractories eroded).

Evaluation results are shown in Figures 7 and 8. It can be seen that the model generally underpredicts the pad temperatures near the central region. The temperature gradient between peripheral pad thermocouples is also underpredicted. Regarding the sidewalls, the agreement between the measured and calculated temperatures is satisfactory.

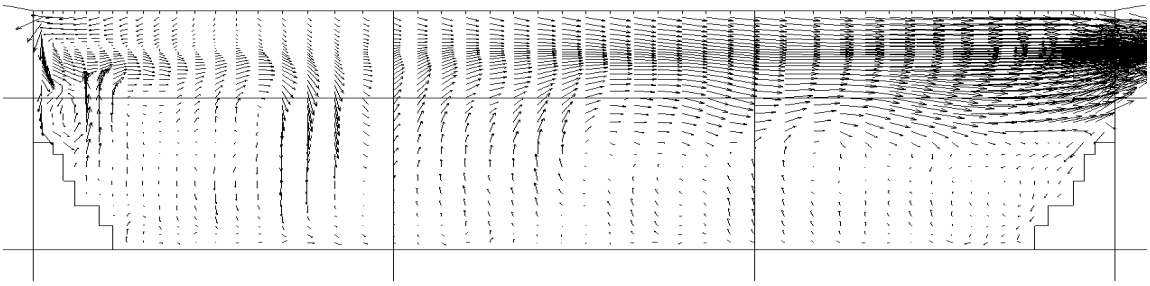

Figure 4: Velocity field in the symmetry plane with original refractory lining.

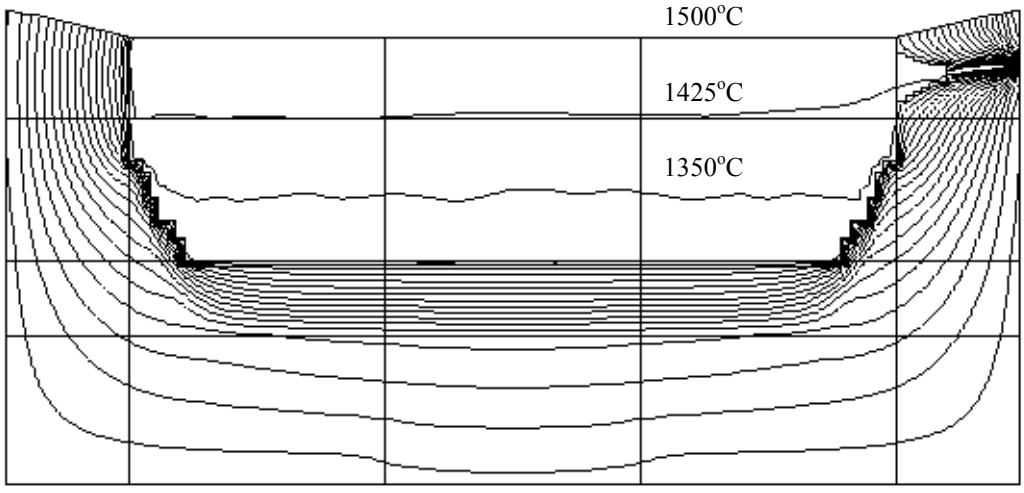

Figure 5: Isotherms in the symmetry plane calculated for hearth with original refractory lining (temperature interval between contours is 75^{o}C).

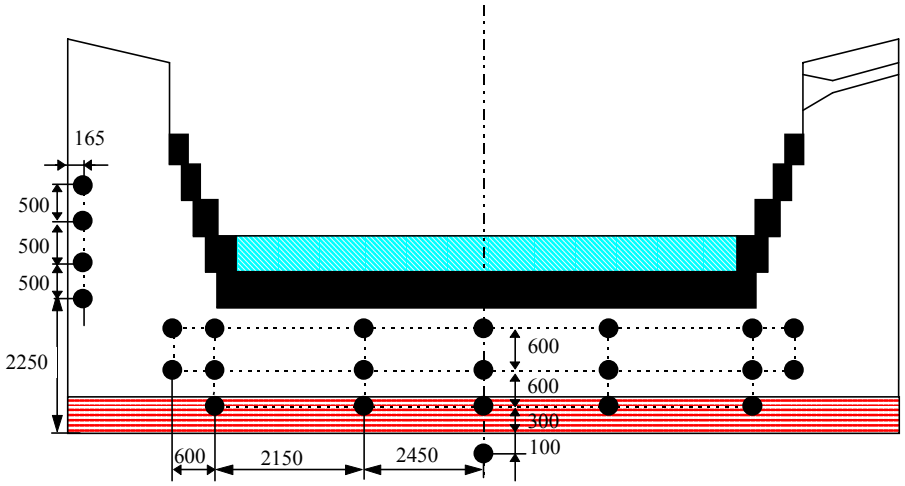

Figure 6: Locations of thermocouples used for evaluation (pad thermocouples are symmetrical around the centreline).

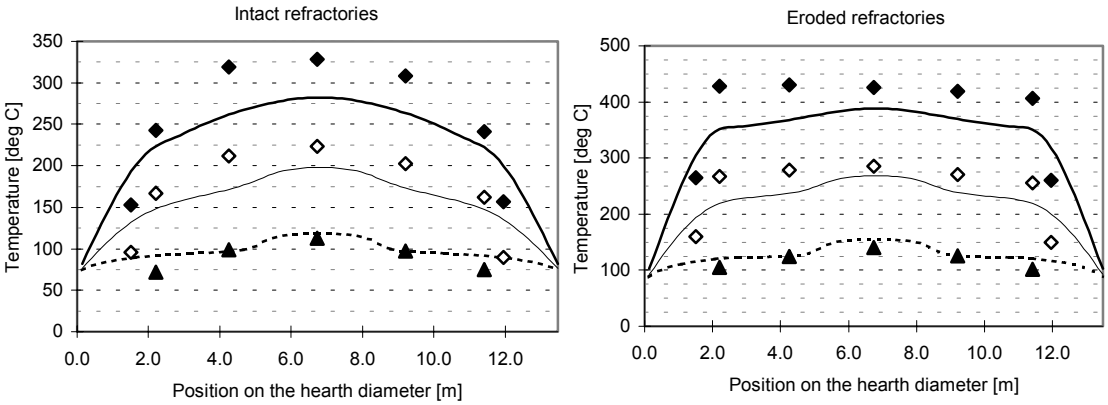

Figure 7: Evaluation with pad thermocouples. Closed diamonds, open diamonds and triangles denote temperatures measured at 1500 mm, 900 mm and 300 mm above the bottom, respectively. Calculated temperatures at the corresponding elevations are denoted with thick and thinner full line and the dashed line, respectively.

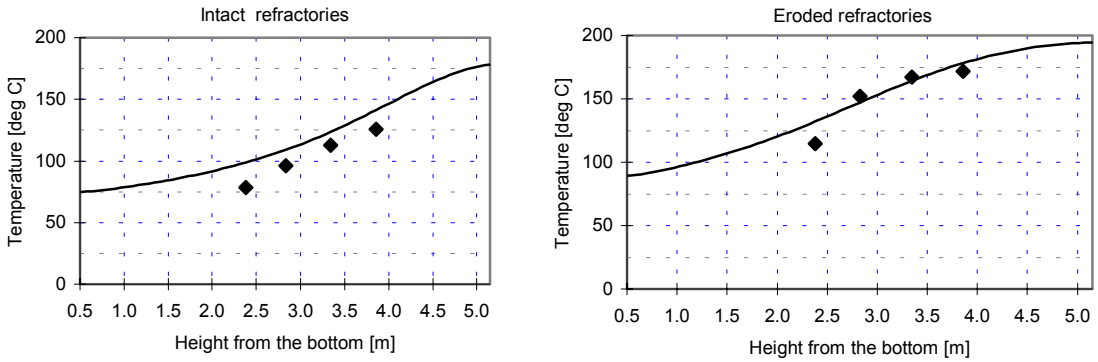

Figure 8: Evaluation with sidewall thermocouples (diamonds denote measured temperatures).

Sensitivity Tests

In order to establish the causes of the discrepancy between the measured and calculated temperatures, and to investigate the parameters that can be used most effectively for hearth wear control, a large number of sensitivity tests have been carried out. These included the physical properties of iron, deadman and refractories (inlet temperature, viscosity, thermal conductivity, porosity). Spatial variations of porosity and boundary temperatures were also examined along with the simulations of various operational conditions (floating deadman, coke-free gutter around the circumference of the hearth well, partial erosion of refractories, production rate). In summary, the most likely causes of discrepancy are:

1. Deadman porosity is larger than assumed (particularly near the walls and bottom). Increased porosity would lead to higher temperatures near the refractory walls, due to higher convective heat transfer;
2. Deadman is floating. Under certain circumstances, still subject to research (Tsuchiya et al., 1998), deadman can be lifted. Liquid iron follows the path of least resistance and a significant portion flows under the deadman.
3. Erosion of refractories is greater than assumed. This would also increase heat losses to the walls and temperatures near the thermocouples.
4. Thermal conductivity of refractories is not accurately known under actual conditions. It is not likely that the firebrick conductivity, which is less accurately known than the rest, is a cause, since after its erosion the discrepancy is about the same magnitude.
5. The spatial variations of temperatures on the cold face of refractories could lead to a better estimate of the temperature gradient between the peripheral thermocouples in the pad.

CONCLUSION

A computational fluid dynamics (CFD) model of the iron flow and heat transfer in a blast furnace hearth has been developed using the commercial package CFX 4.2. The model has been evaluated and the results are generally satisfactory. It has been already used as a tool to assess furnace conditions and interpret observations. Generally, the model underpredicts temperature in the centre of the hearth pad, as well as the gradient in the pad area closer to the walls. The agreement in the sidewalls is good. The likely causes of the discrepancy between measured and calculated temperatures are (a) deadman porosity is larger than assumed, (b) deadman is floating, (c) erosion of refractories is greater than assumed, (d) knowledge of thermal conductivity of refractories is not accurately known under actual conditions, and (e) the spatial variations of the temperatures on the cold face of refractories.

ACKNOWLEDGEMENTS

This work was carried out with the support of BHP Steel. The authors wish to thank BHP Steel for permission to publish this paper.

REFERENCES

CFX 4.2 Flow Solver User Guide, AEA Technology, Harwell, UK, 1997.

GRAY, D.D. and GIORGINI, A. (1976), "The Validity of the Boussinesq Approximation for Liquids and Gases", *Int.J. Heat Mass Transfer*, **19**, 545-51.

IWAMASA, P.K., CAFFERY, G.A., WARNICA, W.D. and ALIAS S.R. (1997), "Modelling of Iron Flow, Heat Transfer, and Refractory Wear in the Hearth of an Iron Blast Furnace", *Int. Conf. On CFD in Minerals&Metal Processing and Power Generation, Melbourne*, 285-95.

KOWALSKI, W., BACHOHOFEN, H.-J., RUETHER, H.-P., ROEDL, S., MARX, K., and THIEMANN, T. (1998), "Computations and Measurements of Liquids Flow in the Hearth of the Blast Furnace", *Proc. 57th ISS-AIME Ironmaking Conf.*, Toronto, 595-606.

KURITA, K. and OGAWA, A. (1994), "A Study of Wear Profile of Blast Furnace Hearth Affected by Fluid Flow and Heat Transfer", *Proc. 1st Int. Cong. of Science and Tech. of Ironmaking,* ISIJ, Sendai, 284-89.

LEPRINCE, G., STEILER, J.M., SERT, D. and LIBRALESSO, J.M. (1993), "Blast Furnace Hearth Life: Models for Assessing the Wear and Understanding the Transient Thermal States", *Proc. 52nd ISS-AIME Ironmaking Conf.*, Dallas, 123-32.

PREUER, A., WINTER, J., and HIEBLER, H. (1992), "Computation of the Iron Flow in the Hearth of a Blast Furnace", *Steel Res.*, **63**, 139-46.

SHA, W.T., YANG, C.I., KAO, T.T. and CHO, S.M. (1982), "Multidimensional Numerical Modelling of Heat Exchanger", *J. Heat Transfer*, **104**, 417-25.

SHIBATA, K., KIMURA, Y., SHIMIZU, M., and INABA, S. (1990), "Dynamics of Dead-man Coke and Hot Metal Flow in a Blast Furnace Hearth", *ISIJ Int.*, **30**, 208-15.

TAKEDA, K. (1994), "Mathematical Modelling of Pulverised Coal Combustion in a Blast Furnace", PhD thesis, Imperial College, London, UK.

TOMITA, Y. and TANAKA, K. (1994), "Development of the 3-dimensional Numerical Model to Estimate Hot Metal Flow and Heat Transfer Behavior at the Blast Furnace Hearth", *Proc. 1st Int. Cong. of Science and Tech. of Ironmaking,* ISIJ, Sendai, 290-95.

TSUCHIYA, N., FUKUTAKE, T., YAMAUCHI, Y. and MATSUMOTO, T. (1998), "In-furnace Conditions as Prerequisites for Proper Use and Design of Mud to Control Blast Furnace Taphole Length", *ISIJ Int.*, **38**, 116-25.

VENTURINI, M.J., BOLSIGNER, J.P., IEZZI, J., and SERT, D. (1998), "Computations and Measurements of Liquids Flow in the Hearth of the Blast Furnace", *Proc. 57th ISS-AIME Ironmaking Conf.,* Toronto, 615-22.

YOSHIKAWA, F. and SZEKELY, J. (1981), "Mechanism of Blast Furnace Hearth Erosion", *Ironmaking and Steelmaking*, **8**, 159-68.